

# Artificial Transmission Line Loaded Dual-polarized Electrically Small Antenna for Wireless Applications

Mohammad Ameen<sup>\*(1)</sup>, and Raghvendra Kumar Chaudhary<sup>(2)</sup>

<sup>(1),(2)</sup>Department of Electronics Engineering, Indian Institute of Technology (Indian School of Mines), Dhanbad, India  
<sup>(1)</sup>mohammadmn61@gmail.com, and <sup>(2)</sup>raghvendra.chaudhary@gmail.com

## Abstract

This paper describes the design of a tri-band and dual-polarized electrically small ( $ka = 0.44$ ) antenna. The antenna is based on the artificial transmission line (ATL) metamaterial (MTM) structure for miniaturization purpose. Due to this, the proposed antenna obtains a compact dimension of  $23.7 \times 25 \times 1.52 \text{ mm}^3$  with an electrical size of  $0.09 \lambda_0 \times 0.10 \lambda_0 \times 0.006 \lambda_0$  at 1.23 GHz. The antenna exhibits triple-band behavior at 1.23 GHz (1.18–1.29 GHz), 4.25 GHz (3.56–4.94 GHz) and 7.76 GHz (6.33–9.20 GHz) with a percentage impedance bandwidths (IBW) of 8.94%, 32.47% and 36.98% for the three bands. Also, the antenna provides circular polarization (CP) radiation at 4.10 GHz and 7.25 GHz with ARBW of 1.22% and 25.37% respectively. The antenna provides excellent IBW, dual AR bands, and good radiation performance by maintaining the antenna compactness. Hence, the intended antenna is appropriate for working in L, S, C and X-band applications.

## 1 Introduction

Due to the advanced technology improvements, compact antennas with multiple functionalities are necessary for the modern application systems. Here comes the role of metamaterial (MTM) antennas, based on ATL for device miniaturization with acceptable antenna features, what the current technologies needed for various applications. ATLs supports the design of left-handed structures with many uncommon features not obtainable in the classical right-handed structures [1]. The ATLs can be realized either by composite right/left-handed (CRLH) transmission line (TL) structures [1]–[2], mu-negative structures [3] epsilon-negative structures [4], and or resonant structures by the loading of complementary split-ring resonators (CSRRs), SRRs [5], electric LC loading [6], and so on. There are various types of ATL based single-band and multi-band antennas are depicted in [2]–[5]. These antennas mainly use CSRR and closed ring resonator [5], electric LC loading and electromagnetic band-gap (EBG) ground plane [6], and complementary capacitive loops [7]. Besides the advantage of compactness, the above explained antennas suffer from narrow IBW, smaller gain values, and lower radiation efficiency with a bigger antenna size.

Presently, the CP antennas are gaining great attraction towards industries due to the benefits of flexibility towards the placement of antennas in the transmitter and receiver

**Table 1.** Comparison between the proposed electrically small antenna with currently existing ATL antennas

Ref. No.	Freq. (GHz)	Antenna size (mm <sup>3</sup> )	ka value	IBW (%)	ARBW (%)	Gain (dBi)
[8]	1.95	24.8 × 22 × 1.6	0.67	1.28	–	-6.9
	2.61			5.3	0.7	-1.1
[9]	1.85	70 × 70 × 3.175	1.91	0.49	NA	-0.24
	2.86			1.33	NA	-0.51
[10]	2.89	60 × 60 × 3.175	2.56	2.94	0.41	6.26
	3.825			0.62	0.9	6.97
[11]	1.38	115 × 115 × 7	2.34	2	–	2
	1.57			1	1.27	7
[12]	1.33	70 × 70 × 2.5	1.37	1.88	–	2.1
	1.8			3.24	–	0.6
	2.41			10.03	1	5.7
Prop.	1.23	23.7 × 25 × 1.52	0.44	8.94	–	-2.3
	4.25			32.47	1.22	3.5
	7.76			36.98	25.37	6.6

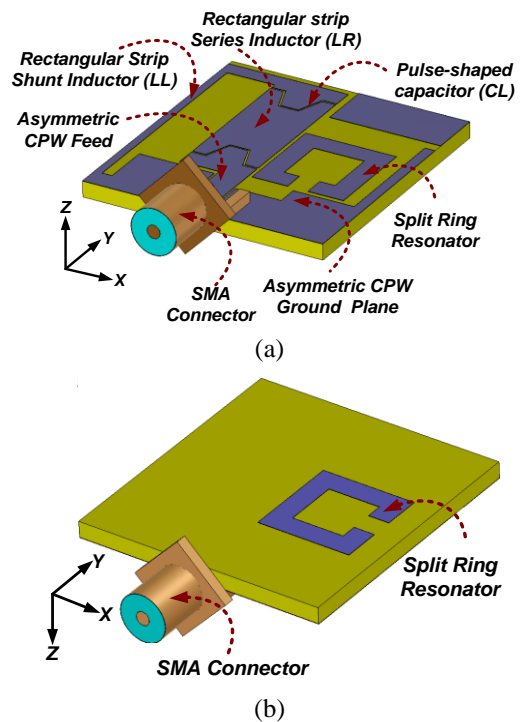


**Figure 1.** 3D view of the proposed ATL based electrically small antenna (a) Front view, and (b) back view.

Side [2]. Various number of CP antennas are explained in [8]–[12]. These antennas use methods such as CRLH-TL

with SRR loading [8], Mushroom with curved branches [9], ENG-TL based CRLH mushrooms [10] for obtaining CP radiation with reduced size. Most of the above-explained antennas fail to deliver essential amount of IBW and gain required for the current application systems. The techniques such as loading of metasurfaces [11] and EBG [12] structures with the radiating antenna can enhance the antenna performance. These antenna minimizes the use in current technologies because the antennas are bulky. So the only solution is to design a low-profile and smaller size antenna with better radiation performance compared with the existing antennas [8]–[12] in the literature.

In this work, a low-profile and miniaturized dual-polarized ATL loaded antenna is designed. The antenna miniaturization is accomplished due to the zeroth-order resonance (ZOR) mode of ATL. Also, multiple bands are obtained due to the addition of SRR structures and asymmetric ground plane. Table. 1 depicts the comparison between the proposed and existing ATL based antennas.

## 2 Proposed Antenna Geometry and Design

The 3D view and schematic look of the intended ATL loaded antenna with corresponding CRLH-TL elements are marked is pictured in Figure 1 and Figure 2 respectively. The presented antenna is simulated using on Rogers TMM4 substrate of  $\epsilon_r = 4.5$ ,  $\tan\delta = 0.002$ , and height  $h = 1.52$  mm. The antenna basically use asymmetrical co-

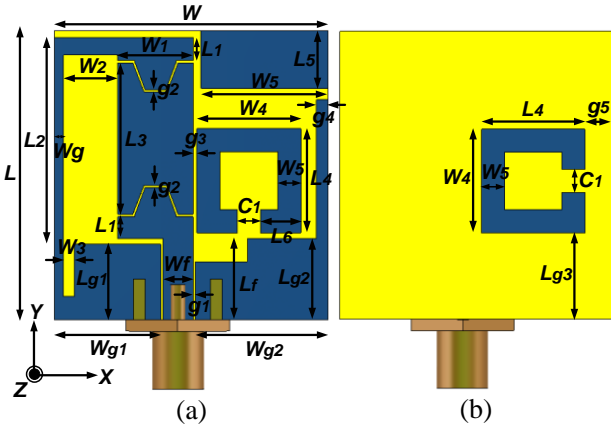


**Figure 2.** Schematic look of the ATL loaded triple-band antenna with dimensions (a) Front view, and (b) back view.

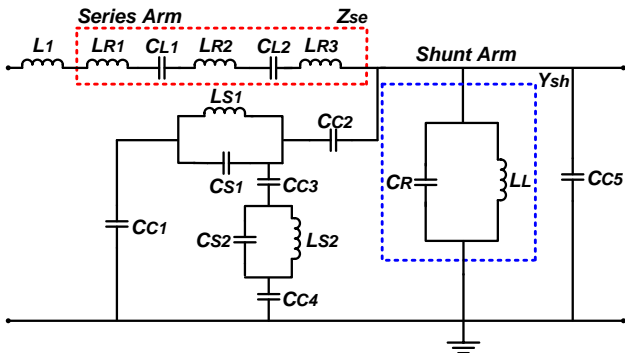


**Figure 3.** Approximate circuit model of the presented electrically small antenna.

planar waveguide (CPW) feeding scheme for achieving wider IBW and CP radiation. The antenna uses microstrip feed line of length  $L_f = 7$  mm and width  $W_f = 2.6$  mm. Also, two asymmetric ground planes ( $W_{g1} \times L_{g1}$  and  $W_{g2} \times L_{g2}$ ) are introduced between the feed line and directly connected to the ATL line. The ATL basically consists of a series inductor ( $L_R$ ), series capacitor ( $C_L$ ), shunt inductor ( $L_L$ ) and shunt capacitor ( $C_R$ ) [1]. The approximate circuit model of the presented electrically small antenna is depicted in Figure 3. Here in the proposed design, the small rectangular strip ( $W_1 \times L_1$ ) introduces a series inductor  $L_{R1}$  as depicted in Figure 3, the pulse-type slot ( $g_2$ ) introduces the series capacitor  $C_{L1}$ , the rectangular strip ( $W_1 \times L_3$ ) introduces series inductor  $L_{R2}$ , the inverted pulse type slot ( $g_2$ ) generates capacitance  $C_{R2}$  and further, the rectangular strip ( $W_1 \times L_1$ ) introduces series inductance  $L_{R3}$  completes the series arm of the ATL. Here the series inductance  $L_R = L_{R1} + L_{R2} + L_{R3}$  and capacitance  $C_L = (C_{L1} \times C_{L2}) / (C_{L1} + C_{L2})$ . The shunt arm consists of a rectangular strip ( $W_g \times L_2$ ) that provides the shunt inductance  $L_L$  and the coupling between the microstrip feed and asymmetric ground ( $W_{g1} \times L_{g1}$ ) provides the shunt capacitance ( $C_R$ ), which completes the shunt arm of ATL. Further introducing different bands, a compact SRR inspired from [2] is introduced in the antenna top side and an additional SRR of same dimension introduced beneath the topside SRR. In the equivalent circuit diagram, the series inductor ( $L_I$ ) represents the feed line of the antenna. For generating multiple bands and CP generation, the additional SRR is introduced in the top side generates capacitor ( $C_{S1}$ ) and inductor ( $L_{S1}$ ). The backside SRR generates capacitor ( $C_{S2}$ ) and inductor ( $L_{S2}$ ). The capacitor  $C_{C1}$ ,  $C_{C2}$ ,  $C_{C4}$ , and  $C_{C5}$  is due to the coupling between the radiator antenna, asymmetric ground, and SRR. The antenna simulations are carried out using CST microwave studio. After several optimizations, the entire dimensions of the antenna is  $23.7 \times 25 \times 1.52$  mm<sup>3</sup> with overall electrical dimensions including asymmetric ground plane is  $0.09 \lambda_0 \times 0.10 \lambda_0 \times 0.006 \lambda_0$  at 1.23 GHz. The final dimensions of the intended antenna are  $L_{g1} = 6.5$ ,  $L_{g2} = L_f = 7$ ,  $L_{g3} = 7.5$ ,  $L_I = 1.8$ ,  $L_2 = 18.1$ ,  $L_3 = 13$ ,  $L_4 = 9$ ,  $L_5 = 5$ ,  $L = 25$ ,  $W = 23.7$  mm,  $W_{g1} = 9.2$  mm,  $W_{g2} = 11.5$  mm,  $W_g = 0.75$ ,  $W_1 = 6.5$ ,  $W_2 = 4.65$ ,  $W_3 = g_4 = 1$ ,  $W_4 = 9$ ,  $W_5 = 11$ ,  $W_f = 2.6$ ,  $g_1 = g_2 = 0.2$ ,  $g_3 = 0.35$ ,  $g_5 = 2.35$ , and  $C_1 = 2$  (All dimensions are in mm).

## 3 ATL Behavior of the Proposed Antenna

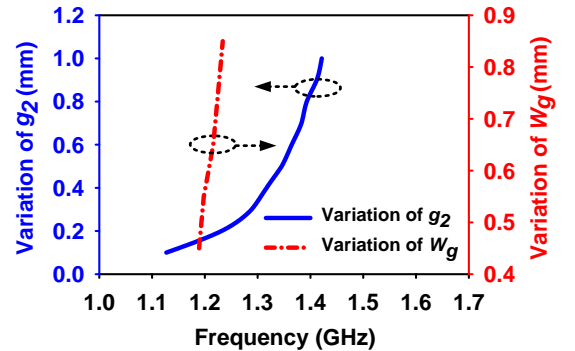


**Figure 4.** Parametric studies on  $S_{11}$  for the series element ( $C_L$ ) and shunt element ( $L_L$ ) of the intended antenna.

To confirm the left-handed behavior of ATL loaded antenna, a parametric investigation is done by varying the shunt and series elements ( $L_L$  and  $C_L$ ) as depicted in Figure 4. It is observed that the ZOR is changing by varying  $g_2$  values from 0.1 mm to 0.9 mm. Also, Figure 4 labels the change in shunt inductor ( $L_L$ ) by varying the  $Wg = 0.45$  mm to 0.85 mm and it is observed that there is no variation in ZOR. Hence, it is proved that the ZOR is obtained by changing the series parameter ( $C_L$ ) and not the shunt parameter ( $L_L$ ) [1].

## 4 Results and Discussions

The simulated 10-dB IBW for the triple-band ATL loaded antenna is 110 MHz (1.18–1.29 GHz), 1380 MHz (3.56–4.94 GHz), and 2870 MHz (6.33–9.20 GHz) with an equivalent fractional bandwidths of 8.94%, 32.47% and 36.98% at the mid frequencies of 1.23 GHz, 4.25 GHz, and 7.76 GHz respectively as depicted in the Figure 5(a). The antenna second and third band provides CP radiation performance at 4.10 GHz and 7.25 GHz. An ARBW of 50 MHz (4.07–4.12 GHz) and 1840 MHz (6.33–8.17 GHz) with a percentage ARBW of 1.22% and 25.37% is obtained as displayed in Figure 5(a). Figure 5(b) shows the gain plot of the intended electrically small antenna. The intended antenna provides a peak gain of -2.3 dBi, 3.5 dBi, and 6.6 dBi at the frequencies of 1.26 GHz, 3.95 GHz and 8.5 GHz respectively. Also, Figure 5(b) represents the efficiency of the antenna. The intended antenna shows an efficiency better than 86% for the three frequency bands.

Figure 6(a) to 6(d) demonstrates the 2D radiation characteristics of the proposed ATL loaded antenna at  $yz$ - and  $xz$ -plane for 1.23 GHz, 4.1 GHz, 7 GHz and 8 GHz respectively. For 1.23 GHz, the intended electrically small antenna demonstrates bidirectional radiation response in

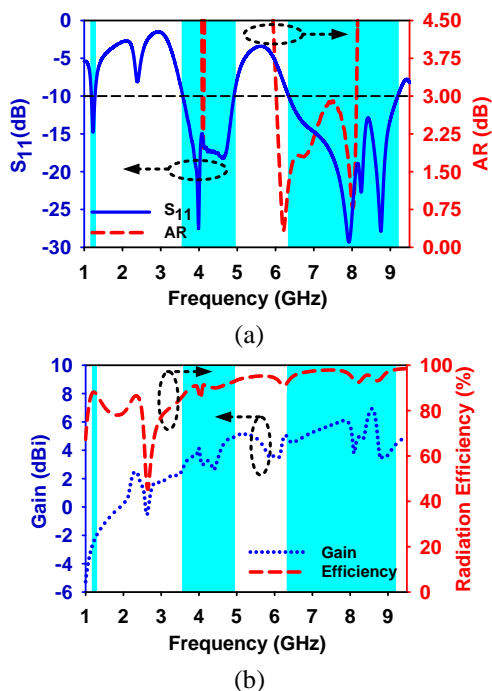


**Figure 5.** Proposed antenna results (a)  $S_{11}$  and AR, (b) Gain and radiation efficiency.

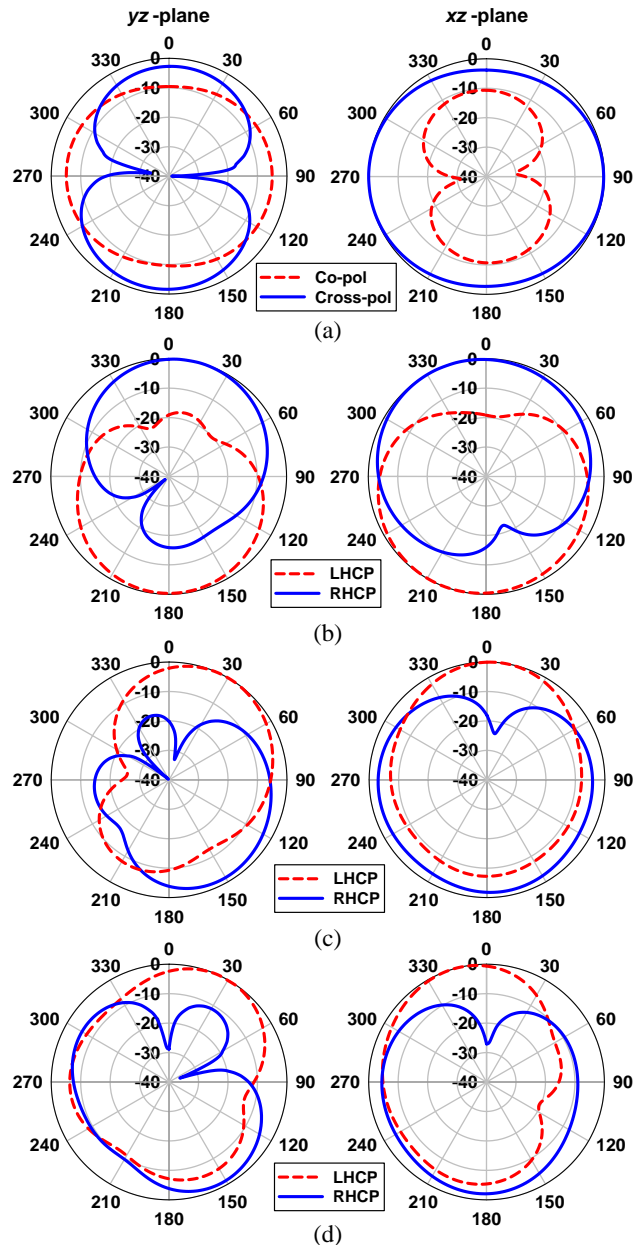


**Figure 6.** Simulated 2D radiation patterns (a) 1.23 GHz, (b) 4.1 GHz, (c) 7 GHz, and (d) 8 GHz.

$yz$ -plane and nearly circular radiation response observed in the  $xz$ -plane. In the second band at 4.10 GHz, the antenna shows RHCP behaviour in  $+Z$  direction and LHCP behaviour in  $-Z$  direction. In the third band at 7 GHz and 8 GHz, the antenna shows LHCP behaviour in  $+Z$  direction and RHCP behaviour in  $-Z$  direction. Here a minor tilting is noted in the patterns due to the unequal ground plane of the intended antenna.

## 5 Electrically Compact Antenna Analysis

For electrically compact antenna, Chu introduces the Chu limit which is re-explained in [4], which defines the lower bound on  $Q$ -factor and its complete achievable bandwidth ( $FBW_{max}$ ). The  $Q$ -factor and  $FBW_{max}$  are interpreted in equation (1) and equation (2).

$$Q_{min} = \frac{1}{k^3 a^3} + \frac{1}{ka} \quad (1)$$

$$FBW_{max} = \frac{S - 1}{Q_{min} \sqrt{S}} \quad (2)$$

The, the maximum achievable gain of an ESA is found by Harrington bound which is described in [4] as depicted in equation (3)

$$G_{dBi} = 10 \log_{10}((ka)^2 + 2ka) \quad (3)$$

For the intended antenna,  $ka = 0.44 < 1$ , hence the proposed antenna is electrically compact. From the equation (1) and equation (2), for  $S =$  voltage standing wave ratio  $= 2$ , the full obtainable BW is 5.04%, which is 0.56 times more than the simulated BW of 8.94% and maximum gain calculated using (2) is 0.30 dBi.

## 6 Conclusion

A compact and dual-polarized multiband ATL antenna is designed. The intended antenna provides IBWs of 8.94%, 32.47% and 36.98% for the three bands centered at 1.23 GHz, 4.25 GHz, and 7.76 GHz respectively. The multiple CP characteristics achieved due to the asymmetric CPW ground plane and SRR loadings. The antenna achieves a smaller size of  $23.7 \times 25 \times 1.52 \text{ mm}^3$  with an electrical size of  $0.09 \lambda_0 \times 0.10 \lambda_0 \times 0.006 \lambda_0$  at 1.23 GHz. Hence, the intended antenna is applicable for L, S, C and X-band.

## 7 Acknowledgements

This research work is supported by Science and Engineering Research Board (SERB), Department of Science and Technology (DST), Government of India under grant number EEQ/2016/000023.

## 8 References

1. M. Ameen and R. K. Chaudhary, "Metamaterial-Based Wideband Circularly Polarised Antenna with Rotated V-Shaped Metasurface for Small Satellite Applications," *Electron. Lett.*, **55**, 7, April 2019, pp. vol. 365–366. doi: 10.1049/el.2018.7348
2. M. Ameen, S. Kalraiya, R. K. Chaudhary, "Coplanar Waveguide-Fed Electrically Small Dual-Polarized Short-Ended Zeroth-Order Resonating Antenna using  $\Omega$ -shaped Capacitor and Single-Split Ring Resonator for GPS/WiMAX/WLAN/ C-band applications," *Int. J. RF. Microw. Comput. Aided. Eng.*, **29**, 12, December 2019, e21946. doi:10.1002/mmce. 21946
3. B. Park and J. Lee, "Compact Circularly Polarized Antenna With Wide 3-dB Axial-Ratio Beamwidth," *IEEE Antennas Wireless Propag. Lett.*, **15**, June 2016, pp. 410–413, doi: 10.1109/LAWP.2015.2448553
4. M. Ameen and R. K. Chaudhary, "Metamaterial Circularly Polarized Antennas: Integrating an Epsilon Negative Transmission Line and Single Split Ring-type Resonator," *IEEE Antennas Propag. Mag.*, January 2020, doi: 10.1109/ MAP.2019.2950920
5. L. Si, W. Zhu and H. Sun, "A Compact, Planar, and CPW-Fed Metamaterial-Inspired Dual-Band Antenna," *IEEE Antennas Wireless Propag. Lett.*, **12**, March 2013, pp. 305–308. doi: 10.1109/LAWP.2013.2249037
6. K. Li, C. Zhu, L. Li, Y. Cai and C. Liang, "Design of Electrically Small Metamaterial Antenna With ELC and EBG Loading," *IEEE Antennas Wireless Propag. Lett.*, **12**, May 2013, pp. 678–681. doi: 10.1109/LAWP.2013.2264099
7. L. Si, *et.al.*, "A Uniplanar Triple-Band Dipole Antenna Using Complementary Capacitively Loaded Loop," *IEEE Antennas Wireless Propag. Lett.*, **14**, Mar. 2015, pp. 743–746. doi: 10.1109/LAWP.2015.2396907
8. C. Zhou, G. Wang, Y. Wang, B. Zong and J. Ma, "CPW-Fed Dual-Band Linearly and Circularly Polarized Antenna Employing Novel Composite Right/Left-Handed Transmission-Line," *IEEE Antennas Wireless Propag. Lett.*, **12**, September 2013, pp. 1073–1076. doi: 10.1109/LAWP.2013.2279689
9. B. Park and J. Lee, "Dual-Band Omnidirectional Circularly Polarized Antenna Using Zeroth- and First-Order Modes," *IEEE Antennas Wireless Propag. Lett.*, **11**, April 2012, pp. 407–410. doi:10.1109/LAWP.2012.2193550
10. S. Ko, B. Park and J. Lee, "Dual-Band Circularly Polarized Patch Antenna With First Positive and Negative Modes," *IEEE Antennas Wireless Propag. Lett.*, **12**, September 2013, pp. 1165–1168. doi: 10.1109/LAWP.2013.2281320
11. J. Lin, Z. Qian, W. Cao, S. Shi, Q. Wang and W. Zhong, "A Low-Profile Dual-Band Dual-Mode and Dual-Polarized Antenna Based on AMC," *IEEE Antennas Wireless Propag. Lett.*, **16**, August 2017, pp. 2473–2476. doi: 10.1109/LAWP.2017.2724540
12. W. Cao, B. Zhang, A. Liu, T. Yu, D. Guo and X. Pan, "Multi-Frequency and Dual-Mode Patch Antenna Based on Electromagnetic Band-gap (EBG) Structure," *IEEE Trans. Antennas Propag.*, **60**, 12, December 2012, pp. 6007–6012. doi: 10.1109/TAP.2012.2211554